A compact active structural acoustic control method for minimizing radiated sound power

Scott D. Sommerfeldt[1]
Brigham Young University
Dept. of Physics and Astronomy
N249 ESC
Provo, UT 84602

ABSTRACT

Active structural acoustic control is an active control method that controls a vibrating structure in a manner that reduces the sound power radiated from the structure. Such methods focus on attenuating some metric that results in attenuated sound power, while not necessarily minimizing the structural vibration. The work reported here outlines the weighted sum of spatial gradients (WSSG) control metric as a method to attenuate structural radiation. The WSSG method utilizes a compact error sensor that is able to measure the acceleration and the acceleration gradients at the sensor location. These vibration signals are combined into the WSSG metric in a manner that is closely related to the radiated sound power, such that minimizing the WSSG also results in significant attenuation of the sound power. The connection between WSSG and acoustic radiation modes will be highlighted. Computational and experimental results for both flat plates and cylindrical shells will be presented, indicating that the WSSG method can achieve near optimal attenuation of the radiated sound power with a minimum number of sensors.

1. INTRODUCTION

Active structural acoustic control (ASAC) is an important subfield of active noise control.[1-6] ASAC is an active control method where one controls the vibration of the radiating structure but in a manner designed to minimize the radiated sound power from the structure, rather than the vibration of the structure. Thus, it is possible in some scenarios to achieve a significant attenuation of the radiated sound power without significantly attenuating the vibration levels on the structure. Such ASAC methods offer the possibility of more efficient attenuation of the radiated sound.

The sound radiated from a structure can be understood and analyzed using the radiation resistance matrix, which encompasses the coupling between the vibration structure and the surrounding acoustic fluid.[3,7] In the 1990s, analysis of the radiation resistance matrix led to the development of acoustic radiation modes, which consist of the eigenvectors associated with the radiation resistance matrix, and which form an orthogonal set of basis functions that describe the acoustic radiation. At low frequencies, the lowest order radiation mode corresponds to the volume velocity associated with

[1] scott_sommerfeldt@byu.edu

the structure, which led to researchers proposing the minimization of the volume velocity as an effective ASAC approach.[8] However, since the volume velocity only represents a single radiation mode, it is limited in how effectively it can attenuate the radiated sound power.

For active control applications where the desire is to minimize the acoustic energy in the field, previous research outlined the advantages of implementing a control system designed to minimize energy-based quantities. One example of this was the minimization of acoustic energy density for active noise control applications, which was suggested as a method for achieving global attenuation of the sound field in an enclosed field.[9,10] When considering ASAC, it then becomes desirable to implement a control metric that is closely related to the radiated sound power. Further, an ideal metric would also be largely insensitive to sensor location. This would ensure rather uniform performance of the system regardless of where the error sensor(s) is located. The weighted sum of spatial gradients (WSSG) control metric was developed as a possible metric that can achieve both of these objectives.

In the following sections, the WSSG metric will be outlined and its connection to acoustic radiation modes will be shown. Implementation of the WSSG metric into a modified filtered-x algorithm will be presented. The WSSG method will then be applied to two active control applications: 1) minimization of the sound field radiated from a vibrating plate, and 2) minimization of the sound field radiated from a vibrating cylindrical shell.

2. DEVELOPMENT OF THE WSSG METHOD

2.1. WSSG Metric

The WSSG control metric consists of four spatial gradient terms that can be thought of as corresponding to a breathing mode, two rocking modes, and a twisting mode.[11-12] The WSSG metric has been developed for both flat structures (plates) and cylindrical shells, and is given by

$$WSSG_{plate} = \alpha \, w^2 + \beta \left(\frac{\partial w}{\partial x}\right)^2 + \delta \left(\frac{\partial w}{\partial y}\right)^2 + \gamma \left(\frac{\partial^2 w}{\partial x \, \partial y}\right)^2$$

$$WSSG_{shell} = \alpha \, w^2 + \beta \left(\frac{\partial w}{\partial z}\right)^2 + \delta \, \frac{1}{a^2}\left(\frac{\partial w}{\partial \theta}\right)^2 + \gamma \, \frac{1}{a^2}\left(\frac{\partial^2 w}{\partial z \, \partial \theta}\right)^2$$

(1)

where w is the normal structural displacement, a is the radius of the cylindrical shell, x,y are the coordinates of the plate, z,θ are the coordinates of the shell, and α, β, δ, and γ are the set of weights that when applied, yield a rather uniform WSSG field with little spatial variance. This can be seen in Figure 1, which shows the WSSG metric for an unwrapped cylindrical shell, where it can be seen that the WSSG is quite uniform except for right near the drive point in the lower left corner.

It can be seen from Equation 1 that the first term represents the displacement, the next two terms represent the gradient in the two orthogonal directions, and the last term represents a second-order twisting term. To measure and implement the WSSG metric, an array of closely-spaced accelerometers is used which together constitute a single integrated error sensor, as shown in Figure 2. (For implementation, the displacements indicated in Equation 1 can be replaced by accelerations.)
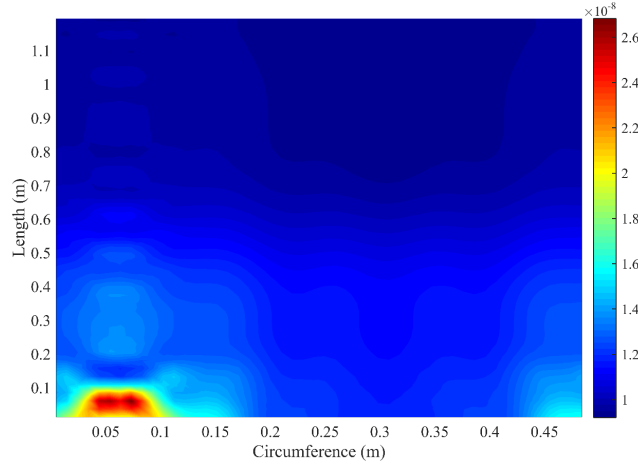
Figure 1. WSSG for a cylindrical shell at a frequency of 541 Hz for the (2,3) mode.
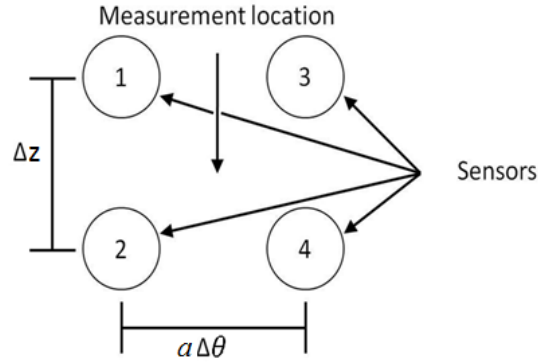

Figure 2. The configuration of four closely spaced sensors (shown here for a cylindrical shell).

With the array of accelerometers, the WSSG can be implemented using the finite difference method, with the terms being represented as (shown for the cylindrical shell)

$$w = \frac{a_1 + a_2 + a_3 + a_4}{4}$$

$$\frac{dw}{dz} = \frac{a_1 - a_2 + a_3 - a_4}{2\Delta z}$$

$$\frac{1}{a}\frac{dw}{d\theta} = \frac{-a_1 - a_2 + a_3 + a_4}{2a\Delta\theta} \tag{2}$$

$$\frac{1}{a}\frac{d^2w}{dzd\theta} = \frac{-a_1 + a_2 + a_3 - a_4}{a\Delta z\Delta\theta},$$

where a_i is the signal from the ith accelerometer.

2.2. WSSG and Acoustic Radiation Modes

A review of the acoustic radiation modes can give some insight into the mechanisms that lead to global attenuation of the radiated sound field. For a vibrating structure, the radiated sound power can be expressed as[7]

$$P(\omega) = \mathbf{v}_e^H(\omega)\mathbf{R}(\omega)\mathbf{v}_e(\omega). \tag{3}$$

Here, the structure has been discretized into small elementary radiators and $\mathbf{v}_e$ is a vector of the velocity of each elementary radiator, $(\bullet)^H$ is the Hermitian transpose, and ω is the frequency of interest. $\mathbf{R}$ is the radiation resistance matrix that relates the normal velocity of each elementary radiator to the acoustic pressure response at all other elementary radiators. The eigenvectors of $\mathbf{R}$ yield the acoustic radiation modes and the eigenvalues of $\mathbf{R}$ are proportional to the radiation efficiency of their respective radiation modes. Thus, by determining the acoustic radiation modes, the radiated sound power can also be expressed as

$$P(\omega) = \sum_{n=1}^{N} \lambda_n |y_n|^2, \tag{4}$$

where λ_n is the nth eigenvalue, and y_n is the amplitude of the nth radiation mode.

For a flat plate excited at low frequencies, the lowest six acoustic radiation modes can be seen in Figure 3. It should be noted that the radiation modes have a mild frequency dependence and exhibit greater curvature at higher frequencies. However, it will be noted that the first four radiation modes correspond to a piston-type displacement, then rocking in the two orthogonal direction, and finally a twisting mode. Thus, the WSSG terms are essentially local point measurements that mirror the global radiation modes. Similarly, the lowest order radiation modes for a cylindrical shell at low frequency are shown in Figure 4.
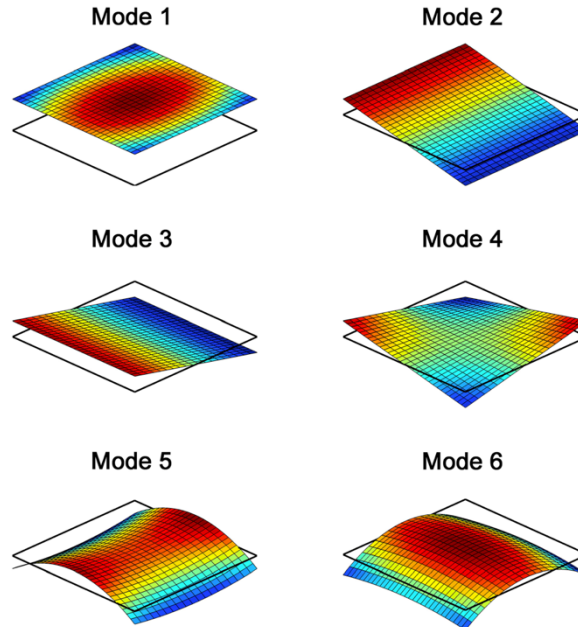

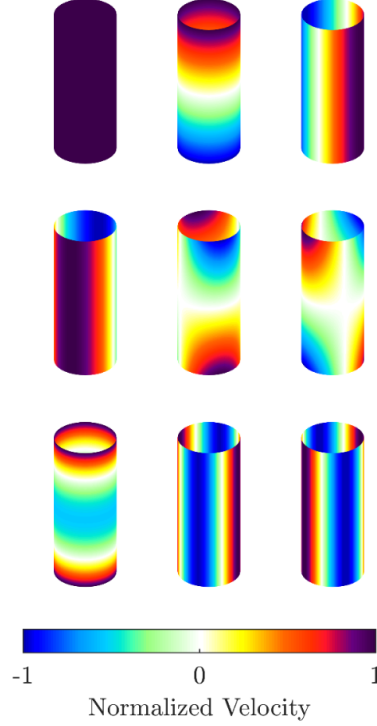Figure 3. The lowest six radiation modes for a flat plate.

Figure 4. The lowest nine radiation modes for a cylindrical shell.

At low frequencies, the acoustic radiation from many structures can be represented in terms of a small number of acoustic radiation modes. The WSSG sensor provides a local estimate of the first four of these radiation modes. Thus, if the structure does not have significant radiation associated with higher radiation modes, the WSSG metric will generally result in very effective global attenuation of the radiated sound power. Furthermore, given the relative uniformity of the WSSG metric over the structure, there is considerable flexibility on where the WSSG sensor is placed.

2.3. Incorporating WSSG into the Filtered-*x* Algorithm

The WSSG metric shown in Equation 1 can be seen to be a quadratic function. As such, a gradient descent method like the filtered-*x* algorithm can be used to minimize that metric. Conceptually, the WSSG metric can be viewed as a sum of four error "signals", corresponding to the four terms of WSSG. Finite difference techniques are used for obtaining these four signals, as shown in Equation 2, resulting in the four "error signals" being given by

$$
\begin{aligned}
e_1 &= \sqrt{\alpha} \left[\frac{d_1 + d_2 + d_3 + d_4}{4} + \mathbf{u}^T \left[\frac{\mathbf{H_1} + \mathbf{H_2} + \mathbf{H_3} + \mathbf{H_4}}{4} \right] \right] \\[2mm]
e_2 &= \sqrt{\beta} \left[\frac{d_1 - d_2 + d_3 - d_4}{2\Delta z} + \mathbf{u}^T \left[\frac{\mathbf{H_1} - \mathbf{H_2} + \mathbf{H_3} - \mathbf{H_4}}{2\Delta z} \right] \right] \\[2mm]
e_3 &= \sqrt{\delta} \left[\frac{-d_1 - d_2 + d_3 + d_4}{2a\Delta\theta} + \mathbf{u}^T \left[\frac{-\mathbf{H_1} - \mathbf{H_2} + \mathbf{H_3} + \mathbf{H_4}}{2a\Delta\theta} \right] \right] \\[2mm]
e_4 &= \sqrt{\gamma} \left[\frac{-d_1 + d_2 + d_3 - d_4}{a\theta\Delta z} + \mathbf{u}^T \left[\frac{-\mathbf{H_1} + \mathbf{H_2} + \mathbf{H_3} - \mathbf{H_4}}{a\Delta\theta\Delta z} \right] \right]
\end{aligned}
\tag{5}
$$

As shown, these expressions are for a cylindrical shell. The corresponding expressions for a flat plate replace Δz with Δx and $a\Delta\theta$ with Δy. In Equation 5, d_i is the primary excitation at each accelerometer and H_i is the transfer function from the control output to each of the four accelerometers, as is routinely implemented for the filtered-x algorithm. This leads to the update equation for the controller as

$$W(t+1) = W(t) - \mu \sum_{i=1}^{4} e_i(t)R_i(t), \tag{6}$$

where R_i is the vector of the current and past values of the ith filtered-x signal, which corresponds to the reference input signal passing through the corresponding H_i transfer function.

3. RESULTS

The WSSG method has been implemented on both flat plate structures, as well as cylindrical shell structures. This section will show some of the computational and experimental results that have been obtained.

3.1. Determining the Weighting Parameters

It can be noted from Equation 1 or Equation 5 that the WSSG metric includes the weighting parameters α, β, δ, and γ, which must be determined before implementing the method. It was stated previously that by properly weighting these parameters, the WSSG metric can be made to be nearly uniform across the structure. The proper values for doing that are related to the structural wavenumbers in the two orthogonal directions and can be expressed as

$$\alpha = 1, \quad \beta = \left(\frac{1}{k_m}\right)^2, \quad \gamma = \left(\frac{1}{k_n}\right)^2, \quad \delta = \left(\frac{1}{k_m k_n}\right)^2, \tag{7}$$

where k_m and k_n are the wavenumbers in the two orthogonal directions of the structure.[13] These wavenumbers are frequency and mode dependent, so several methods of determining the optimal values to use over the entire frequency range have been investigated, including averaging over the bandwidth, using the values for the nearest structural mode, and expressing the wavenumber in terms of the parameters of the structure (bending stiffness, density, thickness). The performance difference in using the various weighting schemes is generally not very significant, since they are all tied to the use of the structural wavenumbers.

3.2. Control of a Flat Plate

The WSSG method was implemented to control the sound power radiated from a flat simply-supported plate.[13] The plate was an aluminum plate with dimensions ($L_x \times L_y$) of 0.473 m $\times$ 0.753 m, thickness (h) of 0.003 m, Young's modulus (E) of 68.9 GPa, and density (ρ) of 2500 kg/m^3. The plate was excited with a disturbance shaker located at (0.445 m, 0.692 m) and was controlled by a second shaker located at (0.422 m, 0.064 m). The WSSG sensor (four accelerometers) was centered at (0.245 m, 0.285 m).

3.2.1 Computational Results

The plate was modelled computationally using MATLAB, and the WSSG method was implemented to predict the effectiveness of the method. Figure 5 shows the results.
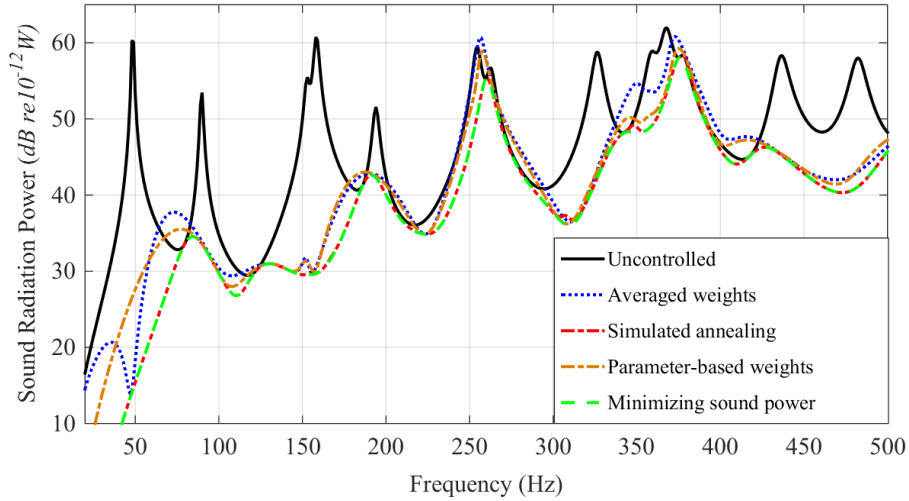
Figure 5. Predicted attenuation of the sound power radiated from a simply-supported plate for the optimal control that minimizes sound power and for several methods of implementing WSSG control.

In Figure 5, since these are computational results, the optimal solution for attenuating the radiated sound power can be obtained and it is shown as the green dashed curve. The simulated annealing curve is a method that can be done computationally which determines the optimal WSSG weights frequency by frequency. It can be seen that it achieves near-optimal control, although it is not a practical control strategy for experimental implementation. The results for averaged weights and parameter-based weights are two methods of determining average values for the WSSG weighting parameters. It can be seen that the performance is generally similar for both choices and that the attenuation is close to the optimal solution at most frequencies. For the frequency range shown here, the optimal sound power attenuation is 15.5 dB, while an attenuation of 14.0 dB is obtained using parameter-based weights and 10.9 dB using averaged weights. The primary difference in performance occurs near 350 Hz. It should be noted that one of the reasons why the WSSG control is not always optimal is that a fixed set of average weights are implemented over the entire frequency band for the WSSG metric, which means that they will not be optimal at all frequencies.

3.2.2 Experimental Results

An experimental simply-supported plate was constructed that closely matched the parameters used for the computational results. The control results obtained are shown in Figure 6. The sound power was measured using a scanning laser Doppler vibrometer to scan a dense grid of the vibrating plate and then determining the radiated sound power using Equation 3. The frequency resolution is more coarse for the experimental results but it can be observed that there is generally good agreement between the computational and experimental results. It can be observed that the control is not effective in the region of 232 Hz and 303 Hz. In looking at the plate model, it was determined that there are degenerate modes in these frequency regions. Since, there is only a single control shaker, there are not enough degrees of freedom to control the multiple modes that are contributing. To verify this, a second control shaker was implemented (green curve), and it can be seen that control was then achieved.
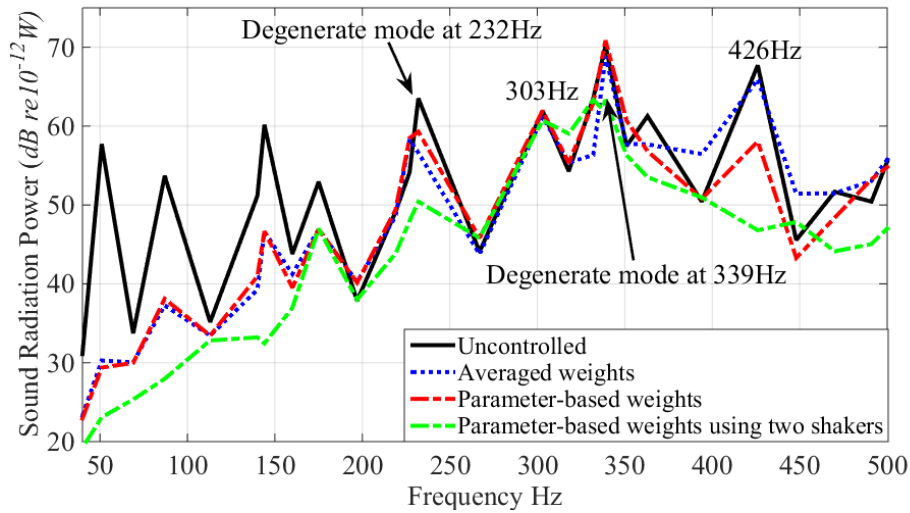
Figure 6. Experimental attenuation of the sound power radiated from a simply supported plate using WSSG control.

3.3. Control of a Cylindrical Shell

The WSSG method was also implemented to control the sound power radiated from a thin cylindrical shell.[12] The shell was again made of aluminum with axial length (L_z) 1.206 m, radius (a) 0.0778 m, and thickness (h) 0.0016 m. For the shaker/sensor locations, the coordinates are given as (z (m), θ (deg)). The shell was excited with a disturbance shaker located at (0.1, 330) and was controlled by a second shaker located at (1.05, 150). The WSSG sensor (four accelerometers) was centered at (0.785, 292).

3.3.1 Computational Results

The cylindrical shell was modelled computationally using MATLAB, and the WSSG method was implemented to predict the effectiveness of the method. Figure 7 shows the results.

The computational results generally predict good attenuation of the radiated sound power. There is a region between 500-800 Hz where some amplification is predicted but over the broad frequency range shown, there is significant attenuation. For this configuration, the computational
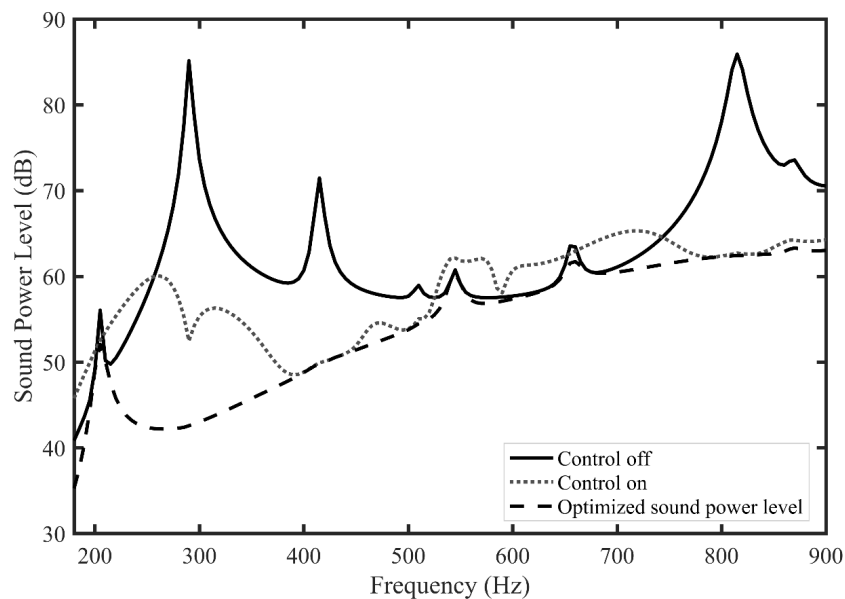

Figure 7. Predicted attenuation of the sound power radiated from a simply-supported cylindrical shell for the optimal control and for implementing WSSG control.

results predict an overall attenuation of 14.0 dB for the optimal control and 11.4 dB for the WSSG method.

The computational results also allow for an investigation of what the control is doing in terms of the acoustic radiation modes. Table 1 shows the amplitudes of the radiation modes without and with control at a frequency of 290 Hz. For this table, the left column provides the amplitudes of the radiation modes without control, the middle column shows the amplitudes with control using the WSSG metric, and the right column shows the amplitudes with control for the optimal control that numerically minimizes the radiated sound power.

Table 1. Radiation mode amplitudes, before and after control, for the ten most efficient radiation modes at 290 Hz.

	S_{bc}	S_{ac}	S_{ac-opt}
Mode 1	-1.1676×10^{-3}	-7.0630×10^{-5}	-5.9740×10^{-5}
Mode 2	2.5131×10^{-3}	5.0015×10^{-3}	5.0262×10^{-3}
Mode 3	1.2722×10^{-1}	9.1847×10^{-5}	1.9270×10^{-7}
Mode 4	1.2104	8.6961×10^{-4}	1.8334×10^{-6}
Mode 5	-2.2861×10^{-3}	-4.4339×10^{-3}	-4.4552×10^{-3}
Mode 6	-1.1503×10^{-2}	-2.2310×10^{-2}	-2.2417×10^{-2}
Mode 7	1.7763×10^{-2}	3.5353×10^{-2}	3.5525×10^{-2}
Mode 8	-1.3518×10^{-2}	-2.6905×10^{-2}	-2.7036×10^{-2}
Mode 9	3.1516×10^{-2}	3.1177×10^{-4}	4.7739×10^{-8}
Mode 10	-1.0240×10^{-2}	-1.0130×10^{-4}	-1.5502×10^{-8}

It can be seen that the WSSG control generally does not alter the amplitudes of low-amplitude radiation modes significantly, such as modes 2, and 5, but instead tends to target the high amplitude modes (which give most of the radiation), such as modes 3 and 4, and attenuates them significantly.

3.3.2 Experimental Results

An experimental simply-supported cylindrical shell was constructed that closely matched the parameters used for the computational results. The control results obtained are shown in Figure 8. For these results, the sound power was measured with the shell in a reverberation chamber and using the ISO 3741 standard, both without and with control running. The results are computed and plotted in terms of 1/3-octave bands. The performance trends are fairly similar, although the amount of attenuation obtained experimentally is not as close to the computational results as it was for the flat plate. The overall experimental attenuation was 5.7 dB. One possible explanation for the reduced attenuation, compared to the flat plate, is that there are more radiation modes contributing to the radiated sound power for the cylindrical shell than there were for the flat plate. Nonetheless, there is still a significant amount of attenuation achieved for the sound power radiated from the shell.
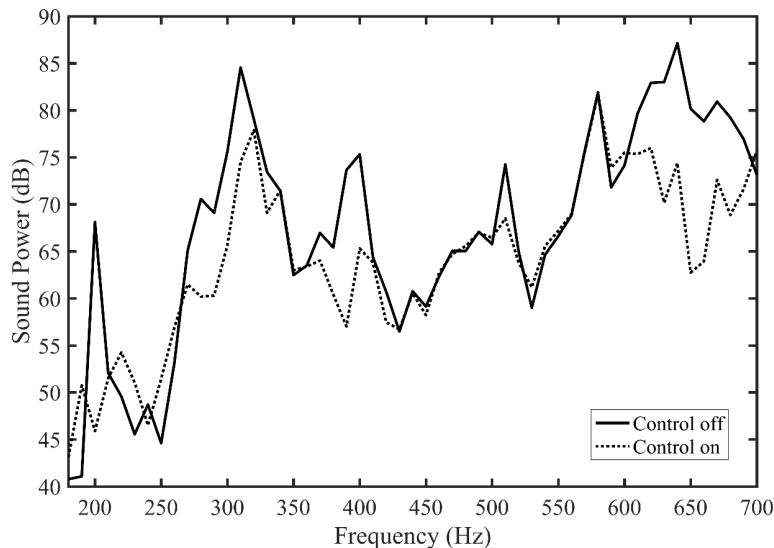
Figure 8. Experimental attenuation of the sound power radiated from a simply supported plate using WSSG control.

4.   CONCLUSIONS

For active noise control applications, it is often effective to focus on developing a method that is closely aligned with what the control objective is. In the case of active structural acoustic control, the desire is to minimize the radiated sound power, so methods that are in some way connected to the radiated sound power will tend to be more effective. The WSSG metric has been introduced as a method that is related to the acoustic radiation modes which can be used to describe acoustic radiation with a relatively small number of terms. WSSG has been shown to be rather uniform over the structure when the weights used are adjusted properly. This means that the sensor is not highly sensitive to sensor location in terms of the control that can be achieved. The WSSG metric is also closely related to acoustic sound power, such that minimizing the WSSG metric will generally lead to good results for attenuating the radiated sound power. Results have been shown for the radiation from flat plates and from cylindrical shells. For flat plates, WSSG often achieves near-optimal attenuation. Results obtained indicate that the attenuation for cylindrical shells is very good but not quite as effective as for flat plates. A primary reason for this result is that the radiation modes for a cylindrical shell exhibit great frequency dependence than for flat plates, and there are typically more modes that contribute to the radiation, so it is difficult to implement a set of fixed weights for the WSSG metric that will be effective at all frequencies. Nonetheless, the results for both types of structures are encouraging and suggest that it is possible to get significant attenuation of the global sound power by minimizing the local WSSG metric.

5.   ACKNOWLEDGEMENTS

6.   REFERENCES

1. Fuller, C. R. Analysis of active control of sound radiation from elastic plates by force inputs. *Proceedings of INTER-NOISE 88*, pp. 1061-1064. Avignon, France, August-September 1988.
2. Fuller, C. R., Hansen, C. H. & Snyder, S. D. Active control of sound radiation from a vibrating panel by sound sources and vibration inputs: An experimental comparison. *Journal of Sound and Vibration,* **145(2)**, 195-216 (1991).

3. Elliott, S. J. & Johnson, M. E. Radiation modes and the active control of sound power. *Journal of the Acoustical Society of America,* **94(4)**, 2194-2204 (1993).

4. Naghshineh, K., Chen, W. & Koopmann, G. H. Use of acoustic basis functions for active control of sound power radiated from a cylindrical shell. *Journal of the Acoustical Society of America* **103(4)**, 1897-1903 (1998).

5. Maillard, J. P. & Fuller, C. R. Active control of sound radiation from cylinders with piezoelectric actuators and structural acoustic sensing. *Journal of Sound and Vibration* **222(3)**, 363-387 (1999).

6. Loghmani, A. Danesh, M., Kwak, M. K. & Keshmiri, M. Active structural acoustic control of a smart cylindrical shell using a virtual microphone. *Smart Materials and Structures* **25(4)**, 045020 (2016).

7. Fahy, F. & Gardonio, P. *Sound and Structural Vibration: Radiation, Tranmission and Response*, 2nd Edition, Elsevier, 2007.

8. Johnson, M. E. & Elliott, S. J. Active control of sound radiation using volume velocity cancellation. *Journal of the Acoustical Society of America,* **98(4)**, 2174-2186 (1995).

9. Sommerfeldt, S. D. & Nashif, P. J. An adaptive filtered-*x* algorithm for energy-based active control. *Journal of the Acoustical Society of America*, **96(1)**, 300-306 (1994).

10. Faber, B. M. & Sommerfeldt, S. D. Global active control of energy density in a mock tractor cabin *Noise Control Engineering Journal*, **43(3)**, 187-193 (2006).

11. Hendricks, D. R., Johnson, W. R., Sommerfeldt, S. D. & Blotter, J. D. Experimental active structural acoustic control of simply supported plates using a weighted sum of spatial gradients. *Journal of the Acoustical Society of America*, **136(5)**, 2598-2608 (2014).

12. Aslani, P., Sommerfeldt, S. D. & Blotter, J. D. Active control of simply-supported cylindrical shells using the weighted sum of spatial gradients control metric. *Journal of the Acoustical Society of America,* **143(1)**, 271-280 (2018)

13. Cao, Y., Sommerfeldt, S. D., Johnson, W., Blotter, J. D. & Aslani, P. An analysis of control using the weighted sum of spatial gradients in active structural acoustic control for flat panel. *Journal of the Acoustical Society of America*, **138(5)**, 2986-2997 (2015).